Loss of basement membrane, receptor and cytoskeletal lattices in a laminin-deficient muscular dystrophy

Peter D. Yurchenco[1,*], Yi-Shan Cheng[1], Kevin Campbell[2] and Shaohua Li[1]

[1]Department of Pathology & Laboratory Medicine, UMDNJ – Robert Wood Johnson Medical School, Piscataway, NJ 08854, USA
[2]Howard Hughes Medical Institute, Department of Physiology & Biophysics, University of Iowa College of Medicine, Iowa City, IA 52242, USA
*Author for correspondence (e-mail: yurchenc@umdnj.edu)

Accepted 2 October 2003
Journal of Cell Science 117, 735-742 Published by The Company of Biologists 2004
doi:10.1242/jcs.00911

Summary

Basement membrane laminins bearing the α2-subunit interact with α-dystroglycan and β1-integrins, cell-surface receptors that are found within the rectilinear costameric lattices of skeletal muscle sarcolemma. Mutations of the α2 subunit are a major cause of congenital muscular dystrophy. To determine whether the costameres are altered as a result of laminin α2-mutations, the skeletal muscle surface of a dystrophic mouse (*dy^{2J}*/*dy^{2J}*) lacking the α2-LN domain was examined by confocal and widefield deconvolution immunomicroscopy. Although the *dy^{2J}* dystrophic fibers possessed a normal-appearing distribution of α2-laminins and α-dystroglycan within a rectilinear costameric lattice at 6.5 weeks of age, by 11 weeks the surface architecture of these components were found to be disorganized, with frequent effacement of the circumferential and longitudinal lattice striations. The defect in the lattice organization was also noted to be a characteristic of type IV collagen, nidogen, perlecan, β1$_D$-integrin, dystrophin and vinculin. The development of this pattern change occurring only after birth suggests that although α2-laminins are not essential for the initial assembly of the costameric framework, they play a role in maintaining the stability and organization of the framework.

Key words: Dystroglycan, Costamere, Muscular dystrophy, Basement membrane

Introduction

The sarcolemmal basement membrane is a plasma membrane-associated extracellular matrix that receives the lateral transmission of contractile force generated by the myofibrils and that participates in the linkage between adjacent and aligned myotubes (reviewed by Bloch et al., 2002; Sanes, 2003). Laminin-2 (α2β1γ1) and laminin-4 (α2β2γ1) are major components of these basement membranes, forming surface-associated polymers through short-arm LN domain interactions and adhering to the cell surface through their G-domains (reviewed by Colognato and Yurchenco, 2000). Receptor interactions of laminin G-domain in muscle include those of dystroglycan and the α7β1 integrin. α-Dystroglycan is bound to its transmembrane moiety β-dystroglycan, and β-dystroglycan binds to dystrophin and other members of the dystrophin-glycoprotein complex (Durbeej et al., 1998; Michele and Campbell, 2003). The laminin-interacting integrin of muscle, α7β1, is also thought to bridge laminin to the underlying cytoskeleton and may provide protective compensation in muscular dystrophies (Burkin et al., 2001; Hodges et al., 1997).

An important class of human congenital muscular dystrophy has been found to be caused by point mutations, deletions or complete absence of the laminin α2 subunit (reviewed by Miyagoe-Suzuki et al., 2000). Several mouse strains containing α2 mutations serve as animal models for the disease (Kuang et al., 1998; Miyagoe et al., 1997; Sunada et al., 1995). Among these, the murine *dy^{2J}* dystrophy has been shown to result from an in-frame deletion within the N-terminal globular domain of the laminin α2 subunit (Sunada et al., 1995; Xu et al., 1994) that destabilizes the domain and renders it unable to polymerize (Colognato and Yurchenco, 1999; Guo et al., 2003). The dystrophy is characterized by degeneration and regeneration of muscle fibers. Modestly decreased levels of laminin α2 have been detected by immunofluorescence in the sarcolemmal surfaces of these mice, with irregular attenuations of the basement membrane seen at the ultrastructural level (Colognato and Yurchenco, 2000; Sunada et al., 1995; Xu et al., 1994). Similarly, variable loss of the α2 subunit, near-normal levels of type IV collagen, and compensation by other laminin α-subunits have been appreciated in other laminin-α2 deficient states (Kuang et al., 1998; Patton et al., 1999; Sunada et al., 1994).

Mature skeletal muscle fibers possess a rectilinear framework called the costamere, which is thought to be responsible for linking the tightly packed and aligned contractile myofibers to the sarcolemma and basement membrane (Bloch et al., 2002). The costameric framework consists of major repeating circumferential bands of receptors and cytoskeletal components that are aligned with the myofibril Z-line (Z-elements), minor repeating circumferential lines interspersed between the Z-elements (M-elements), and parallel longitudinal striations (L-elements). Vinculin, spectrin, β1-integrin, dystroglycan and laminins have all been found to

be concentrated at, or largely confined to, the elements of the costameric array, suggesting that these components are all connected to each other and linked to the myofibers Z- and M-discs by desmin and other proteins. The array has been found to be a dynamic structure whose major axis of alignment is sensitive to denervation and muscle agrin (Bezakova and Lomo, 2001).

Recently, it was found that α1- and α2-laminins were found to organize dystroglycan, integrin α7β1, vinculin and dystrophin into irregular polygonal arrays in cultured myotubes produced by the fusion of mouse satellite cell-derived C2C12 myoblasts, possibly constituting precursor structures to the rectilinear costameres seen in adult muscle (Colognato et al., 1999). The changes produced by the addition of exogenous laminins to the culture medium were found to require both its polymerization and G-domain-mediated cell-surface binding. Because the LN domain of laminin that is involved in polymerization is defective in the *dy*^{2J} mouse, because laminin extracted from *dy*^{2J} is unable to induce the polygonal array in myotubes (Colognato et al., 1999; Colognato and Yurchenco, 1999), and because the same components organized by laminin into the C2C12 polygonal array are also found in costameric arrays, it seemed that a defect in the costameric array might be found in the skeletal muscle of the *dy*^{2J} mouse. We therefore examined the surface distribution of basement membrane, cell surface and several cytoskeletal components in normal and *dy*^{2J} mouse muscle. We report that basement membrane, receptor and cortical cytoskeletal lattice patterns appear initially normal in *dy*^{2J} muscle but become distorted and effaced by 11 weeks of age. Our findings suggest that although α2-laminins contribute to the stability of the array, they are not uniquely essential for its formation.

Materials and Methods

Antibody and protein reagents

Rabbit polyclonal antibodies specific for type IV collagen, the core protein of perlecan, the G domain of the laminin α2 chain, and placental laminins-2/-4 were prepared and characterized as described previously (Cheng et al., 1997; Handler et al., 1997; Rambukkana et al., 1998; Yurchenco and Ruben, 1987). Polyclonal antibody for nidogen-1 (entactin-1) was generated by immunizing a New Zealand white rabbit with protein purified from the EHS (Engelbreth-Holm-Swarm) laminin-nidogen complex. Purification was accomplished by dissociating nidogen from laminin in 2 M guanidine-HCl in 50 mM Tris-HCl, pH 7.4, 2 mM EDTA on ice and separating the species by two rounds of gel filtration with Sephacryl S-500 (90 cm × 2.5 cm column) in the same buffer. The antiserum was affinity purified with nidogen immobilized on Sepharose 4B beads and then cross-absorbed on nidogen-free laminin immobilized on Sepharose beads. Mouse monoclonal IgM antibody IIH6 hybridoma medium specific for α-dystroglycan (Ervasti and Campbell, 1991) was used as conditioned hybridoma medium or purified from medium. Rabbit polyclonal antibody specific for dystrophin was prepared against a dystrophin fusion protein as described previously (Ervasti et al., 1990). Mouse monoclonal IgG antibody 2B1 (van der Flier et al., 1997) specific for the integrin $\beta1_D$ chain was kindly provided by Arnoud Sonnenberg (Netherlands Cancer Institute). Mouse monoclonal anti-rabbit α-actinin and mouse monoclonal anti-chicken vinculin antibodies were purchased from Sigma (St Louis, MO). FITC-, Cy3- and Cy5-conjugated antibodies specific for mouse IgG, mouse IgM and rabbit IgG, respectively, were purchased from Jackson Immunochemicals (Bar Harbor, ME).

Preparation and immunostaining of skeletal muscle

Breeding pairs of heterozygous C57BL/6J-*Lama 2*$^{dy\text{-}2J}$ mice and homozygous C57BL/10ScSn *mdx/mdx* mice (4-6 weeks of age) were obtained from Jackson Laboratory (Bar Harbor, ME) and housed in the medical school vivarium and treated under an animal protocol approved by the Institutional Animal Care and Use Committee. Homozygous *dy*^{2J}/*dy*^{2J} offspring and their normal littermates were distinguished from each other by the presence or absence of a distinct gait abnormality that primarily affects the hind limbs. Following anesthetization of mice injected intraperitoneally with 0.05 ml of a 6.5% solution of sodium pentobarbital, the chest cavity was exposed, the left ventricle of the heart cannulated with a 25 gauge 'butterfly' syringe needle, the right atrium incised and the animal perfused for several minutes with phosphate buffered saline (10 mM sodium phosphate, 127 mM NaCl, pH 7.4) followed by a 1.5-1.8% solution of paraformaldehyde in phosphate buffered saline for 20 minutes. Hind limb muscles were exposed by dissection and prepared for microscopy following teasing, or, for a limited number of samples, cryostat sectioning. Excised portions of muscle were slowly teased with fine forceps into individual fibers and fiber groups and adhered onto glass slides. For cryostat sectioning, a portion of muscle was rapidly plunge-frozen in a propane slush cooled to liquid nitrogen temperatures using a pneumatic-driven plunger. Sections 10-20 μm thick were cut in a Leica CM1850 cryostat at –18°C. Slides were post-fixed in 1.5% paraformaldehyde in phosphate buffered saline for 10-20 minutes. Following fixation, slides were either used detergent-free or treated with 0.5% Triton-X-100 in phosphate buffered saline for 30 minutes on ice. They were then blocked with 0.5% bovine serum albumin in phosphate buffered saline at 5°C, incubated with primary antibodies (anti-laminin-α2G or anti-laminin-2/-4, 20 μg/ml; anti-type IV collagen, perlecan or nidogen, 10 μg/ml, anti-dystroglycan IIH6 conditioned medium, undiluted or 1:1 dilution; anti-integrin $\beta1_D$ conditioned medium without dilution; anti-vinculin and anti-dystrophin, 1:20 dilution; anti-α-actinin, 1:400 dilution) diluted in blocking buffer. After washing, the slides were incubated with secondary antibody conjugated to FITC, Cy3 or Cy5 according to the manufacturer's instructions for 1.5 hours at room temperature. Nonimmune mouse IgM, mouse IgG and rabbit IgG were used as controls. The slides were again washed over a 2 hour period. Nuclei were stained with a 10 μg/ml solution of propidium iodide (viewed with a Chroma narrow X HQ TRITC filter set) or stained with 2 μg/ml DAPI. The latter was found to provide better tissue penetration. Coverslips were mounted with 6% 1,4 diazabicyclo(2,2,2)octane (Sigma) in a 9:1 mixture of glycerol:100 mM Tris-HCl, pH 8.6 to inhibit photobleaching.

Light microscopy and analysis of digital images

Digital confocal images were obtained with either a Zeiss LSM 410 Invert laser scanning microscope fitted with a 63× oil immersion objective (NA=1.4) and capable of discriminating among FITC, TRITC/Cy3 and Cy5 fluorescence, or an Olympus IX81 inverted microscope fitted with a CARV confocal imaging device, PCO SensiCam CCD camera, 60× oil immersion objective (NA=1.4) and DAPI, FITC, TRITC/Cy3 and Cy5 filters and controlled by IPLab (Scanalytics, Fairfax, VA). Slides were also viewed by widefield indirect immunofluorescence using an Olympus IX70 inverted microscope fitted with IX-FLA fluorescence observation attachment, 60× oil immersion objective (NA=1.4), and a MicroMax 5 mHz CCD camera (Princeton Instruments, NJ) controlled by IP Lab. For these images, out-of-focus haze was reduced by digital deconvolution of sets of 16, 32 or 64 serial optical sections recorded at 0.25 μm intervals using an expectation maximization algorithm and a calculated point spread function (Conchello and McNally, 1996; McNally et al., 1999) in the program XCOSM (Institute for Biomedical Computing, Washington University, St Louis, MO). Confocal images were processed in Adobe Photoshop (San Jose, CA)

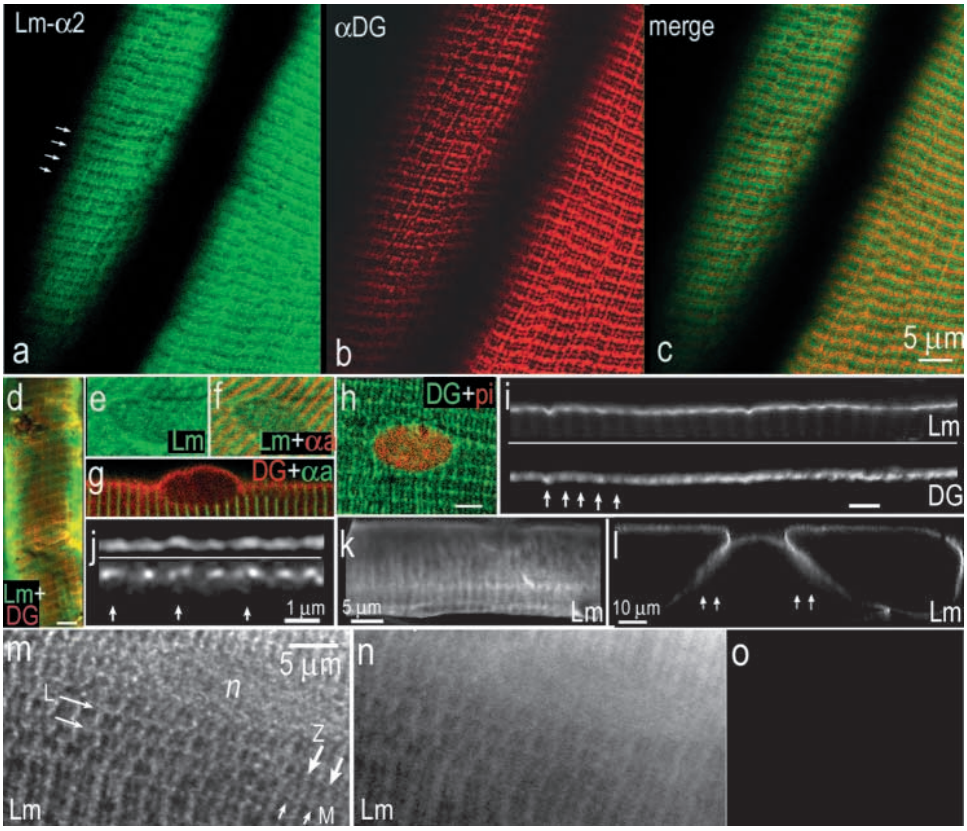

Fig. 1. Laminin (Lm) and α-dystroglycan (DG) in normal skeletal muscle. (a-d) Confocal immunofluorescence images of the surface of normal teased muscle fibers immunostained with laminin α2-G domain (a, FITC secondary, green) and α-dystroglycan (b, IIH6, Cy3, red) antibodies (a-c, fixed and detergent treated). Laminin and dystroglycan striated patterns colocalize (arrows in a), with less intense laminin fluorescence between striations. (d) Similar fiber image with laminin-dystroglycan costained fiber treated with detergent following laminin immunostaining. (e-h) Peripheral nuclei (e, laminin; f, laminin (green) and α-actinin (red); g, oblique optical section showing nucleus protruding beyond plane of sarcolemma (dystroglycan, red; α-actinin, green); h, laminin, green; propidium iodide, red). Peripheral nuclei are sandwiched between α-actinin of the sarcomere (which coincides with the major costameric circumferential striations) and plasma membrane dystroglycan. (i-j) Periodicity of orthogonally oriented longitudinal optical sections (i, confocal image, laminin-2/4 above and α-dystroglycan below; j, deconvoluted widefield image, laminin α2G above and dystroglycan below) of normal fibers. Arrows indicate positions of Z-discs. (k-o) Widefield images reveal repeating pattern of laminin α2G epitope on internal (k,l) and external (m,n) basement membrane surfaces. (k) An oblique view of an internal basement membrane lying between adjacent fibers contained within a computed three-dimensional pixel (voxel) array prepared from 0.25 μm serial deconvoluted optical sections. (l) Location of internal basement membranes within optical cross-section through three adjacent fibers (arrows). (m-o) Images of fixed teased fiber prepared without detergent and stained with laminin α2G-specific antibody following (m) and before (n) deconvolution, and incubated only with secondary antibody (o). Costameric elements (Z, M, L striations) and location of peripheral nucleus (*n*) indicated in m.

and deconvoluted images in IP Labs and, when required, analyzed in three dimensions using Voxblast 3.0 (VayTek, Fairfield, IO).

Results

Sarcolemmal architecture of normal skeletal muscle

The distribution of laminin was examined on teased myotube surfaces with a polyclonal antibody raised against laminin-2/4 and an antibody prepared against the laminin α2 G domain by confocal and widefield deconvolution microscopy (Fig. 1). By either method, and with either reagent, laminin-specific immunofluorescence was present well above background levels over almost the entire surface but was brightest in a regular rectilinear pattern that consisted of alternating broad and narrow circumferential striations intersected by parallel longitudinal lines. The major circumferential striations had a periodicity of 2.2±0.2 μm (mean ± standard deviation, n=26), and the overall pattern was similar to that of the costamere. The prominence of the striations varied somewhat from fiber to fiber, with the intercostameric regions having intensities typically less than a one quarter below that of the brightest regions as measured in IPLab. When laminin immunofluorescence was examined as confocal or deconvoluted longitudinal oriented orthogonal optical sections, the periodic difference in intensity was also noted, but it was less than that for images prepared en face. The laminin pattern array was observed in both detergent-permeabilized and nonpermeabilized fibers, and in both teased fibers and frozen sections of muscle, indicating that the structure was independent of these manipulations.

Strikingly, the rectilinear laminin pattern colocalized with a similar but generally more contrasted array of α-dystroglycan in both its major circumferential and longitudinal striations. Many laminin and dystroglycan costained or independently stained images also revealed the existence of finer (minor) circumferential lines lying between the major striations in the laminin-stained images, corresponding to more prominent inter-Z striations in the dystroglycan-stained images. The Z-line of the laminin and dystroglycan array was established with antibody to α-actinin. Peripheral nuclei, scattered on the myotube surface, were identified with propidium iodide and DAPI (see below), often projected beyond the sarcolemmal plane. Oblique views and serial sections revealed that the laminin and dystroglycan extended over the outer surface of the nuclei while α-actinin, marking the sarcomere, lay beneath. The laminin and dystroglycan costameric patterns in teased fibers were examined in quadraceps femoris and soleus at 6.5 weeks, and

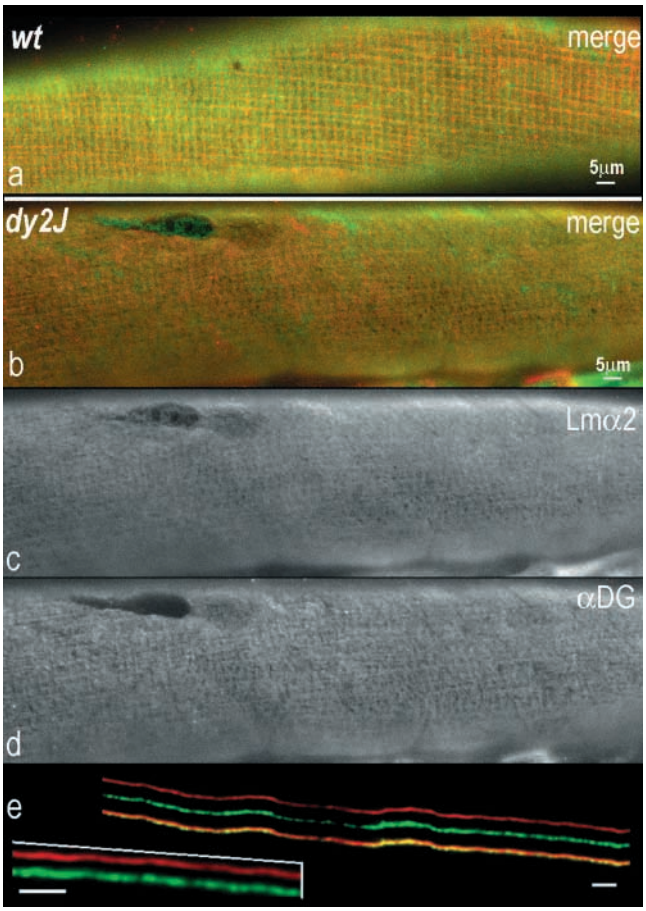

Fig. 2. Defects in the surface organization of laminin and dystroglycan in dy^{2J} muscle. Confocal images of teased *dy^{2J}* dystrophic muscle fibers (b-e: b, merged image; c, laminin-α2-G; d, α-dystroglycan). A wild-type control fibril (merged image) is shown in a. (e) A deconvoluted widefield cross-sectional view of dystrophic basement membrane zone (dystroglycan, red; laminin, green; merge, yellow). Note extensive (but not complete) effacement of rectilinear distributions for surface-distributed basement membrane, receptor and cytoskeletal components. Bars, 2 μm in e.

quadraceps femoris, adductor magnus, gracilis, soleus and tibialis anterior muscle at 14.5 weeks. The laminin and dystroglycan patterns were found to be continuous or near-continuous in all of these muscles, with about the same degree of variability within a muscle as between them. As shown ahead, basement membrane type IV collagen, nidogen and perlecan were also condensed into a rectilinear pattern. It was concluded that laminin-2 and laminin-4 and other major basement membrane components form a continuous sarcolemma coating but are condensed within an rectilinear array that coincides with that of dystroglycan.

Sarcolemmal surface architecture of laminin-deficient dystrophic skeletal muscle

Skeletal muscle obtained from *dy^{2J}* mice aged 11-12 weeks was examined. The distribution of laminin-α2 and dystroglycan was found to be substantially altered in most fibers (Figs 2-5). Although a faint residual costameric pattern could often still be

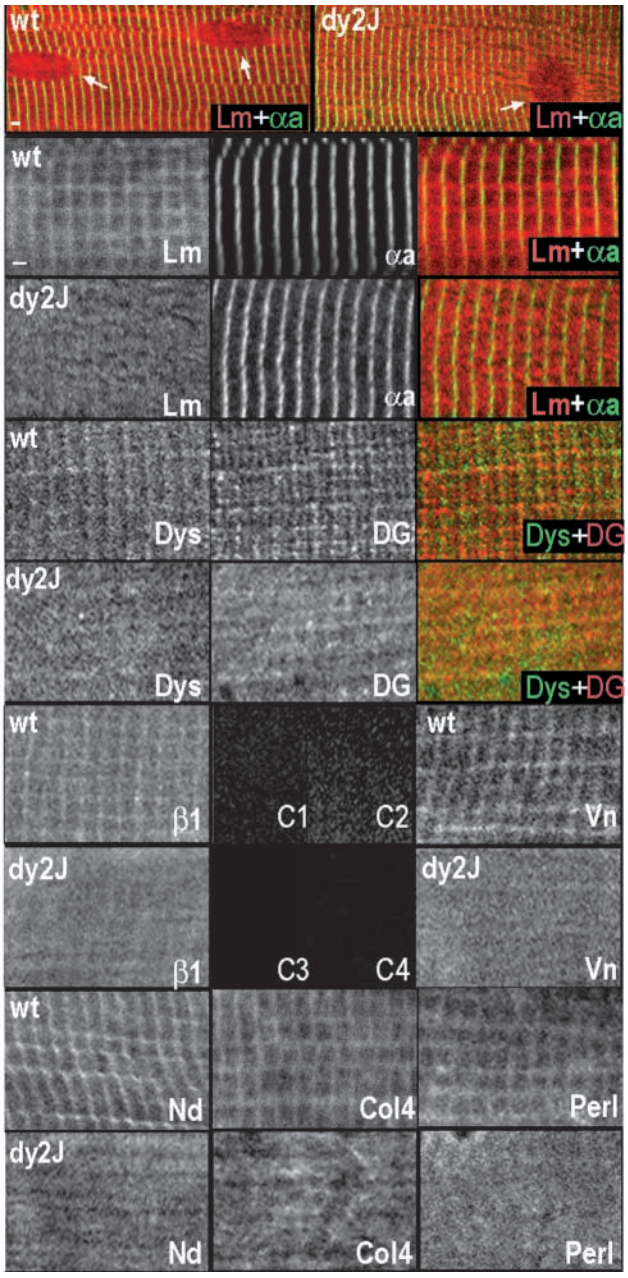

Fig. 3. Defects in the surface organization of basement membrane, receptor and cytoskeletal components in dy^{2J} muscle. Confocal images of wild-type (wt) and dystrophic (dy2J) muscle fibers. Muscle fibers immunostained to detect laminin-α2 (Lm) and corresponding α-actinin (αa), dystrophin (Dys) and corresponding dystroglycan (DG), integrin β1D, vinculin (Vn), nidogen (Nd), type IV collagen (Col4) and perlecan (Perl). Nonimmune (wild-type) controls for integrin (C1), vinculin (C2), dystrophin/basement membrane components (C3) and dystroglycan (C4) included. Note the extensive but incomplete effacement of rectilinear distributions for surface-distributed basement membrane, receptor and cytoskeletal components with preservation of the sarcomeric α-actinin cross-band architecture. Arrows in top row panel indicate locations of peripheral nuclei which overlie the sarcomeres. Bar, 2 μm.

appreciated, the laminin and dystroglycan components were now seen to splay beyond the confines of the lattice, obscuring

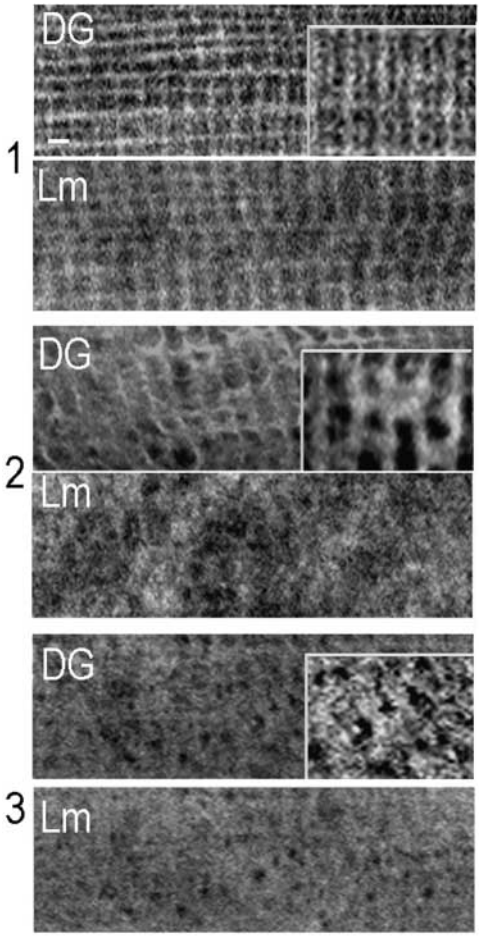

Fig. 4. Grading of normal and dy^{2J} surface architectures. Three classes of surface architecture were defined from the dystroglycan immunofluorescence patterns. Class 1, seen in normal muscle, corresponds to a regular rectilinear pattern. Class 2, largely present in dystrophic muscle, consists of a less regular lattice with splaying and with frequent loss of the finer circumferential and longitudinal lattice struts. Class 3 is a dystrophic pattern characterized by substantial loss of the rectilinear pattern with extensive inter-array clearing (shown) or near-complete pattern effacement. Corresponding paired images with 1.5× magnified insets for dystroglycan shown.

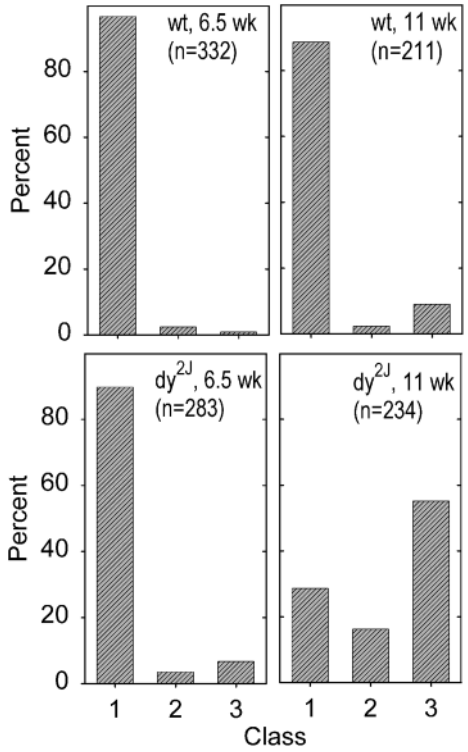

Fig. 5. Age-dependent transitions in dy^{2J} surface architecture. The orthogonal pattern in 6.5-week and 11-week-old *dy^{2J}/dy^{2J}* mice and their normal littermates was scored. Number of determinations (n, image fields) indicated in panels. The class 2 and 3 changes are characteristics of dystrophic muscle, developing after 6.5 weeks.

the normal grid-like pattern and creating a fairly diffuse and sometimes disorganized distribution of epitope (Fig. 2), i.e. the defective fibers possessed varying degrees of effacement of the lattice array pattern both for dystroglycan and laminin. Type IV collagen, nidogen and perlecan were found to possess a surface pattern in normal mouse muscle similar to that for laminin (Fig. 3). This pattern colocalized with that of $\beta 1_D$ integrin receptor, and cytoskeletal dystrophin and vinculin. This pattern was noted to be effaced in *dy^{2J}* muscle for all of these components. By contrast, the pattern of sarcomeric α-actinin was found to remain unchanged with preservation of the evenly spaced parallel Z-bands.

Temporal progression of surface architecture in dy^{2J} dystrophic muscle

Muscles obtained from younger normal and *dy^{2J}* mice (3 weeks, not shown, and 6.5 weeks) were evaluated. The dystroglycan and laminin costameric patterns could not be distinguished from muscle obtained from normal littermates. To quantitate the degree of surface alteration at two ages, muscle fibers were then collected from dystrophic mice aged 6.5 weeks and 11 weeks, and from their normal littermates, and evaluated by confocal microscopy. Gradations of structural abnormality could be appreciated and these were divided into three groups (Fig. 4). Class 1 fibers were defined as fibers with regular lattice patterns, sometimes with a relatively small degree of ligand staining detected beyond the fine rectilinear array. Class 2 fibers were defined as fibers with surfaces characterized by splaying of the pattern accompanied by rounding of the intersections, filament irregularity and/or a piecemeal loss of interlattice segments (particularly the M-line and longitudinal filaments). Class 3 fibers were defined as fibers characterized by extensive loss of the lattice pattern. Some of these surfaces showed preservation of central interlattice clearing, whereas others showed near-complete effacement. As shown (Fig. 5), there was little or no difference seen between normal and dystrophic mice at 6.5 weeks. The normal pattern consisted of ~90% regular orthogonal array. However, profound differences in fiber architecture became evident by 11 weeks of age, i.e. 71% of fiber fields had class 2-3 effacement patterns.

The fraction of central nuclei, an indicator of regenerating and regenerated fibers, was estimated from counts of hematoxylin-stained nuclei and eosin counterstained cross-sections of

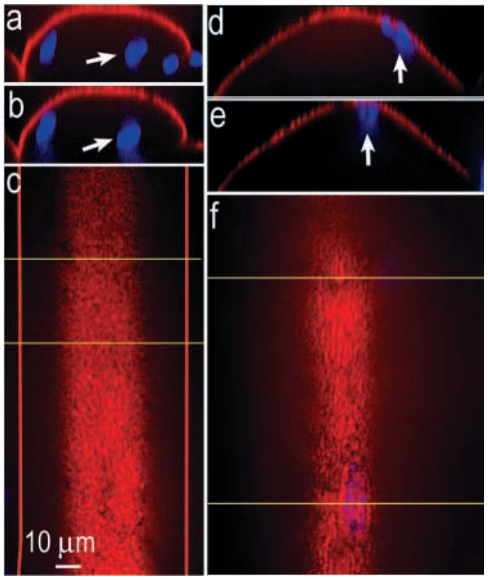

Fig. 6. Loss of costameric lattice in dy^{2J} fibers with central and peripheral nuclei. Confocal images of teased muscle fibers from an 11-week-old *dy^{2J}* dystrophic mouse stained with DAPI (blue) to detect nuclei and with IIH6 antibody (red) to detect α-dystroglycan. Cross-sectional views (a,b; d,e) reconstructed from serial optical 0.5 μm sections taken approximately at positions indicated by yellow lines in en face views of upper surface (c,f). Red vertical lines indicate lateral borders of fiber in c. Note dystrophic pattern seen in myofiber containing central nuclei (a-c) and peripheral nuclei (d-f).

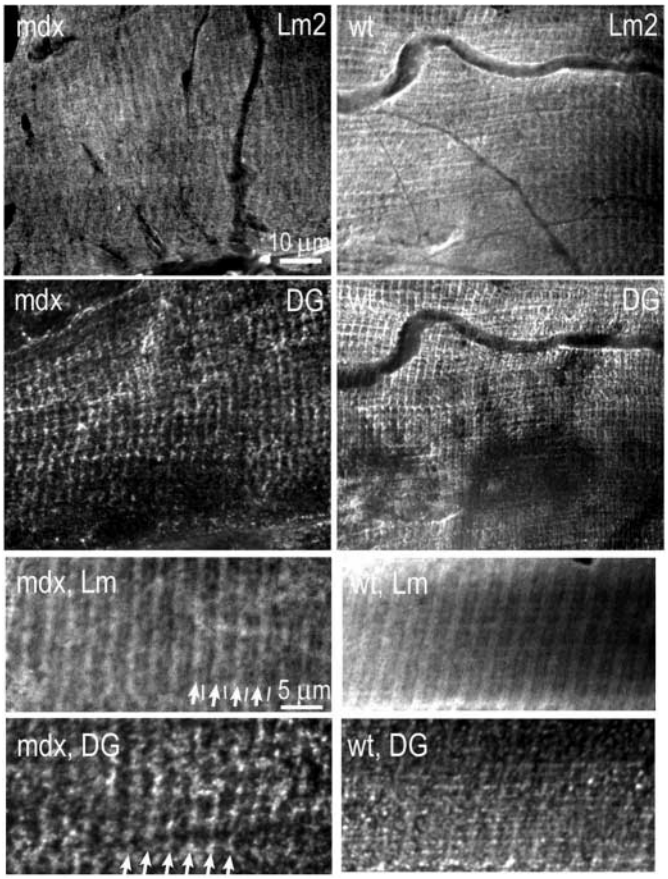

Fig. 7. Surface distribution of laminin-2/4 and α-dystroglycan in mdx dystrophic muscle. Confocal images of teased muscle isolated from an 11-week-old *mdx/mdx* mouse. The pattern of laminin-2/4 (Lm2) revealed prominent Z bands with variable reductions of M- and longitudinal striations, and more prominent selective loss of the α-dystroglycan (DG) inter-Z minor circumferential M bands. The furrows are sites of capillaries removed from the sarcolemma.

contralateral hindlimb muscle. They were found to be 2% of normal 6.5-week-old muscle (74/3173 nuclei), 6% of *dy^{2J}/dy^{2J}* 6.5-week muscle (250/4254), 1% of normal 11-week-old muscle (108/10767) and 21% of *dy^{2J}/dy^{2J}* 11-week muscle (1957/9542). Increased variation in fiber diameter was noted at 11 weeks. The basement membrane laminin and dystroglycan patterns appeared essentially normal at 6.5 weeks and markedly abnormal at 11 weeks, with the fraction of affected fibers exceeding the fraction containing central nuclei. Both thin and thick 11-week-old fibers were noted to have altered surface architectures. To determine whether the costameric alterations developed in regenerated muscle fibers that contain central nuclei, and 'primary' fibers that contain peripheral nuclei, 11-week-old dystrophic fibers and fiber groups were stained with DAPI to detect nuclei and immunostained with dystroglycan-specific and laminin-2/4-specific antibodies to determine the costameric pattern (Fig. 6). Serial optical sections were used to generate en face views, and orthogonal z-sections were computationally obtained from these. Fibers containing both peripheral and central nuclei were identified. The surface of both fiber types showed effacement of the normal costameric pattern. Collectively, these data suggest that the fibers that present initially at birth, as well as regenerating myofibers, had been affected.

Sarcolemmal surface architecture of dystrophin-deficient skeletal muscle

The pattern of laminin and α-dystroglycan on fibers teased from 11-week-old homozygous *mdx* mice was compared with age-matched controls (Fig. 7). The dystrophic fibers exhibited an altered costameric dystroglycan pattern in which the minor circumferential bands (corresponding to the M-line) and longitudinal striations were reduced in intensity, absent, or irregular, similar to those reported for spectrin in older skeletal muscle of the *mdx* mouse (Williams and Bloch, 1999). The circumferential M-line and longitudinal striations of the laminin pattern were reduced compared with normal in areas overlying abnormal dystrophic striations.

Discussion

In the present study we found that basement membrane α2-laminins, type IV collagen, nidogen and perlecan are organized as continuous sarcolemmal sheets containing rectilinear condensations that coincide with the costameric lattice of α-dystroglycan, β1 integrin, dystrophin and vinculin. This lattice becomes disorganized in the *dy^{2J}* mouse between 6.5 and 11 weeks of age such that the circumferential and longitudinal condensations are disrupted and/or extend beyond their normal linear borders, obscuring the normal architecture. The pattern is different from the M-line and longitudinal striation defects seen in age-matched *mdx* mouse muscle (Fig. 8).

Previously, we found that laminin-1 and laminin-2 can

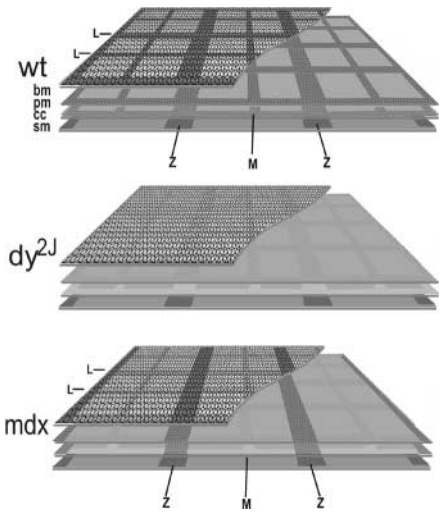

Fig. 8. Model of normal and dystrophic costameric patterns. Sarcolemmal basement membrane (bm), plasma membrane (pm), cortical cytoskeleton (cc) and underlying sarcomeres (sm) are shown. Normal (wild-type, wt) basement membrane, although continuous, is condensed into circumferential Z (major) and M (minor) bands and longitudinal (L) striations that correspond to the same pattern elements seen with β1-integrin and dystroglycan receptors and cytoskeletal vinculin and dystrophin. The basement membrane, receptor and cytoskeletal *dy*^{2J} lattice-like patterns become generally effaced while the receptor (dystroglycan, this study) and cytoskeletal (spectrin) (Williams and Bloch, 1999) M and L elements of *mdx* muscle are lost, with less-pronounced changes in the laminin pattern.

organize dystroglycan, integrin, dystrophin and vinculin into an irregular polygonal array in cultured myotubes (Colognato et al., 1999), the same components found in the rectilinear costameric framework. Although it is not known whether this irregular polygonal array is a precursor to the costamere, the organization of shared components into distinct surface architectures argues for a relationship between the two entities. One possibility is that the irregular polygonal architecture of cultured myotubes is not organized in a rectilinear array simply because the sarcomeres are too sparse and too well separated from the plasma membrane to allow components such as desmin to effectively form a bridge between the sarcomeric Z-disc and sarcolemma, as is thought to be the case in mature muscle (Bloch et al., 2002).

It has been proposed that the costameric arrays are the sites of force transmission and that these forces stabilize membrane and cytoskeletal costameric components (Danowski et al., 1992; Sharp et al., 1997). Because a basement membrane forms a coat around each myotube with fusion occurring between adjacent fibers, mechanical forces transmitted between myotubes during contraction must be transmitted across the adjacent basement membranes through the costameric portion. Defects arising in the array appear to be deleterious for muscle function; one such change has been evident in the *mdx* mouse, a model for muscular dystrophies with defects in dystrophin in which partial compensation is provided by utrophin (Grady et al., 1997). In the *mdx* mouse, the array defect is characterized by a loss of spectrin and other components over M lines and in the longitudinal strands of the lattice array (Williams and Bloch, 1999), and we found a similar pattern for dystroglycan in these mice as early as 11 weeks of age.

In the *dy*^{2J} mouse, the α2-laminin subunit is deleted within the LN domain (Sunada et al., 1995). Although defective in self-assembly, the α2-laminins nonetheless remain within basement membranes, probably tethered through nidogen, agrin, integrin, dystroglycan and other cell-surface binding molecules (Colognato and Yurchenco, 1999). The defective laminins, unlike native laminin-1 or laminin-2, were unable to induce a polygonal array of receptors and cytoskeleton in cultured myotubes, which suggests that laminins play an important role in their surface organization (Colognato et al., 1999). 11-week-old *dy*^{2J} dystrophic muscle fibers exhibited an effaced pattern of laminin, receptors and cytoskeletal elements reminiscent of the nonpolymerization state seen on cultured myotubes after treatment with *dy*^{2J} laminin; however, the normal rectilinear array organization seen in younger mice showed that α2-laminin polymerization cannot be uniquely essential for costameric assembly. Instead, the data argued that α2-laminin polymerization is important for the maintaining the stability of these structures.

However, the broader question of whether *a* laminin is required for costameric assembly remains unresolved. Although the α2 subunit is the major muscle laminin subunit present after birth (Kuang et al., 1999), developing and regenerating skeletal muscle express other laminin α-subunits that associate with the β and γ subunits (Patton et al., 1999). In particular, it has been reported in the severe laminin α2-deficient *dy/dy* mouse that both the laminin α4 and α5 chains are expressed at increased levels during development and regeneration, with increase of the former seen under a variety of pathological conditions (Patton et al., 1999; Ringelmann et al., 1999). Thus, laminin subunit redundancy and compensation exists and may insure a role of laminin in costameric assembly in either the absence of α2 expression, or the expression of defective α2 subunit. A hypothesis to be considered is that in the presence of partial laminin compensation, a lattice structural defect develops early in the dystrophic muscle, which affects stability, but which is morphologically latent. Progression to the morphological defect might require an initiating event that overstresses the weak lattice such as contraction against load, as has been proposed for non-laminin dystrophies (Campbell, 1995).

This work was supported by a grant (NS38469) from the National Institutes of Health (to P.D.Y.). K.P.C. is an Investigator of the Howard Hughes Medical Institute. We thank Andrea Biermann at the Robert W. Johnson Medical School for her technical assistance.

References

Bezakova, G. and Lomo, T. (2001). Muscle activity and muscle agrin regulate the organization of cytoskeletal proteins and attached acetylcholine receptor (AchR) aggregates in skeletal muscle fibers. *J. Cell Biol.* **153**, 1453-1463.

Bloch, R. J., Capetanaki, Y., O'Neill, A., Reed, P., Williams, M. W., Resneck, W. G., Porter, N. C. and Ursitti, J. A. (2002). Costameres: repeating structures at the sarcolemma of skeletal muscle. *Clin. Orthop.* S203-210.

Burkin, D. J., Wallace, G. Q., Nicol, K. J., Kaufman, D. J. and Kaufman, S. J. (2001). Enhanced expression of the alpha7beta1 integrin reduces muscular dystrophy and restores viability in dystrophic mice. *J. Cell Biol.* **152**, 1207-1218.

Campbell, K. P. (1995). Three muscular dystrophies: loss of cytoskeleton-extracellular matrix linkage. *Cell* **80**, 675-679.

Cheng, Y. S., Champliaud, M. F., Burgeson, R. E., Marinkovich, M. P. and Yurchenco, P. D. (1997). Self-assembly of laminin isoforms. *J. Biol. Chem.* **272**, 31525-31532.

Colognato, H. and Yurchenco, P. D. (1999). The laminin alpha2 expressed by dystrophic dy(2J) mice is defective in its ability to form polymers. *Curr. Biol.* **9**, 1327-1330.

Colognato, H. and Yurchenco, P. D. (2000). Form and function: the laminin family of heterotrimers. *Dev. Dyn.* **218**, 213-234.

Colognato, H., Winkelmann, D. A. and Yurchenco, P. D. (1999). Laminin polymerization induces a receptor-cytoskeleton network. *J. Cell Biol.* **145**, 619-631.

Conchello, J. and McNally, J. (1996). Fast regularization technique for expectation maximization algorithm for computational optical sectioning microscopy. In *Three-Dimensional Microscopy: Image Aquisition and Processing III*, Vol. 2655 (ed. C. J. Cogswell, G. S. Kino and T. Wilson), pp. 199-208. Proc. SPIE-The International Society for Optical Engineering.

Danowski, B. A., Imanaka-Yoshida, K., Sanger, J. M. and Sanger, J. W. (1992). Costameres are sites of force transmission to the substratum in adult rat cardiomyocytes. *J. Cell Biol.* **118**, 1411-1420.

Durbeej, M., Henry, M. D. and Campbell, K. P. (1998). Dystroglycan in development and disease. *Curr. Opin. Cell Biol.* **10**, 594-601.

Ervasti, J. M. and Campbell, K. P. (1991). Membrane organization of the dystrophin-glycoprotein complex. *Cell* **66**, 1121-1131.

Ervasti, J. M., Ohlendieck, K., Kahl, S. D., Gaver, M. G. and Campbell, K. P. (1990). Deficiency of a glycoprotein component of the dystrophin complex in dystrophic muscle. *Nature* **345**, 315-319.

Grady, R. M., Teng, H., Nichol, M. C., Cunningham, J. C., Wilkinson, R. S. and Sanes, J. R. (1997). Skeletal and cardiac myopathies in mice lacking utrophin and dystrophin: a model for Duchenne muscular dystrophy. *Cell* **90**, 729-738.

Guo, L. T., Zhang, X. U., Kuang, W., Xu, H., Liu, L. A., Vilquin, J. T., Miyagoe-Suzuki, Y., Takeda, S., Ruegg, M. A., Wewer, U. M. et al. (2003). Laminin alpha2 deficiency and muscular dystrophy; genotype-phenotype correlation in mutant mice. *Neuromuscul. Disord.* **13**, 207-215.

Handler, M., Yurchenco, P. D. and Iozzo, R. V. (1997). Developmental expression of perlecan during murine embryogenesis. *Dev. Dyn.* **210**, 130-145.

Hodges, B. L., Hayashi, Y. K., Nonaka, I., Wang, W., Arahata, K. and Kaufman, S. J. (1997). Altered expression of the alpha7beta1 integrin in human and murine muscular dystrophies. *J. Cell Sci.* **110**, 2873-2881.

Kuang, W., Xu, H., Vachon, P. H., Liu, L., Loechel, F., Wewer, U. M. and Engvall, E. (1998). Merosin-deficient congenital muscular dystrophy. Partial genetic correction in two mouse models. *J. Clin. Invest.* **102**, 844-852.

Kuang, W., Xu, H., Vilquin, J. T. and Engvall, E. (1999). Activation of the lama2 gene in muscle regeneration: abortive regeneration in laminin alpha2-deficiency. *Lab. Invest.* **79**, 1601-1613.

McNally, J. G., Karpova, T., Cooper, J. and Conchello, J. A. (1999). Three-dimensional imaging by deconvolution microscopy. *Methods* **19**, 373-385.

Michele, D. E. and Campbell, K. P. (2003). Dystrophin-glycoprotein complex: Post-translational processing and dystroglycan function. *J. Biol. Chem.* **278**, 15457-15460.

Miyagoe, Y., Hanaoka, K., Nonaka, I., Hayasaka, M., Nabeshima, Y., Arahata, K., Nabeshima, Y. and Takeda, S. (1997). Laminin alpha2 chain-null mutant mice by targeted disruption of the Lama2 gene: a new model of merosin (laminin 2)-deficient congenital muscular dystrophy. *FEBS Lett.* **415**, 33-39.

Miyagoe-Suzuki, Y., Nakagawa, M. and Takeda, S. (2000). Merosin and congenital muscular dystrophy. *Microsc. Res. Tech.* **48**, 181-191.

Patton, B. L., Connoll, A. M., Martin, P. T., Cunningham, J. M., Mehta, S., Pestronk, A., Miner, J. H. and Sanes, J. R. (1999). Distribution of ten laminin chains in dystrophic and regenerating muscles. *Neuromuscul. Disord.* **9**, 423-433.

Rambukkana, A., Yamada, H., Zanazzi, G., Mathus, T., Salzer, J. L., Yurchenco, P. D., Campbell, K. P. and Fischetti, V. A. (1998). Role of alpha-dystroglycan as a Schwann cell receptor for Mycobacterium leprae. *Science* **282**, 2076-2079.

Ringelmann, B., Roder, C., Hallmann, R., Maley, M., Davies, M., Grounds, M. and Sorokin, L. (1999). Expression of laminin alpha1, alpha2, alpha4, and alpha5 chains, fibronectin, and tenascin-C in skeletal muscle of dystrophic 129ReJ dy/dy mice. *Exp. Cell Res.* **246**, 165-182.

Sanes, J. R. (2003). The basement membrane/basal lamina of skeletal muscle. *J. Biol. Chem.* **278**, 12601-12604.

Sharp, W. W., Simpson, D. G., Borg, T. K., Samarel, A. M. and Terracio, L. (1997). Mechanical forces regulate focal adhesion and costamere assembly in cardiac myocytes. *Am. J. Physiol.* **273**, H546-556.

Sunada, Y., Bernier, S. M., Kozak, C. A., Yamada, Y. and Campbell, K. P. (1994). Deficiency of merosin in dystrophic dy mice and genetic linkage of laminin M chain gene to dy locus. *J. Biol. Chem.* **269**, 13729-13732.

Sunada, Y., Bernier, S. M., Utani, A., Yamada, Y. and Campbell, K. P. (1995). Identification of a novel mutant transcript of laminin alpha 2 chain gene responsible for muscular dystrophy and dysmyelination in dy2J mice. *Hum. Mol. Genet.* **4**, 1055-1061.

van der Flier, A., Gaspar, A. C., Thorsteinsdottir, S., Baudoin, C., Groeneveld, E., Mummery, C. L. and Sonnenberg, A. (1997). Spatial and temporal expression of the beta1D integrin during mouse development. *Dev. Dyn.* **210**, 472-486.

Williams, M. W. and Bloch, R. J. (1999). Extensive but coordinated reorganization of the membrane skeleton in myofibers of dystrophic (mdx) mice. *J. Cell Biol.* **144**, 1259-1270.

Xu, H., Wu, X. R., Wewer, U. M. and Engvall, E. (1994). Murine muscular dystrophy caused by a mutation in the laminin alpha 2 (Lama2) gene. *Nat. Genet.* **8**, 297-302.

Yurchenco, P. D. and Ruben, G. C. (1987). Basement membrane structure in situ: evidence for lateral associations in the type IV collagen network. *J. Cell Biol.* **105**, 2559-2568.